JOURNAL OF Materials CHEMISTRY

Insights into the formation of hydroxyl ions in calcium carbonate: temperature dependent FTIR and molecular modelling studies

Satish I. Kuriyavar,[a] Rajappan Vetrivel,[a] Sooryakant G. Hegde,[a] Arumugamangalam V. Ramaswamy,[a] Debojit Chakrabarty[b] and Samiran Mahapatra*[b]

[a]*Catalysis Division, National Chemical Laboratory, Pune 411 008, India*
[b]*Unilever Research India, Hindustan Lever Research Centre, I.C.T. Link Road, Andheri(E), Mumbai, 400 099, India*

Received 7th March 2000, Accepted 16th May 2000
Published on the Web 6th July 2000

This paper describes the use of temperature dependent FTIR spectroscopy and molecular modelling studies to establish the origin and the nature of surface hydroxyl ions on calcium carbonate. It has been demonstrated that two types (Type I, corresponding to a band at 3690 cm^{-1} and Type II, corresponding to a band at 3640 cm^{-1}) of hydroxyl ions exist on calcium carbonate surfaces prepared by the carbonation method. Type I hydroxyl ions are ascribed to those of the unreacted calcium hydroxide (portlandite) present due to incomplete carbonation and Type II hydroxyl ions are ascribed to interstitial defects which are strongly associated with the calcium carbonate lattice framework. Interestingly, the calcium carbonate samples prepared by the solution method do not possess Type I/Type II hydroxyl ions. A molecular modelling exercise was carried out to generate the calcite 104 plane, and the different modes of adsorption of water on the calcite 104 plane were derived based on energy minimisation calculations. The possibility of replacement of a carbonate ion either by (i) two hydroxyl ions or (ii) a hydroxyl and a bicarbonate ion has been considered. The replacement of a carbonate ion by one hydroxyl and one bicarbonate ion is indicative of the presence of surface/interstitial defects on calcite (corresponding to Type II hydroxyl ions assigned by FTIR studies). A molecular description of hydroxylating calcite surfaces is discussed in detail and the results from the energy of formation at zero water coverage corroborate the above findings. The calculations also predict the formation of a maximum of two pairs of hydroxyl and bicarbonate ions over a surface area of 1.0 nm^2, during chemisorption at low surface coverages.

Introduction

Calcium carbonate can be precipitated in aqueous solution as three anhydrous polymorphs, calcite, aragonite and vaterite, and three hydrated forms, amorphous calcium carbonate, calcium carbonate hexahydrate and calcium carbonate monohydrate.[1,2] There are two further forms, namely, calcite II and calcite III, which are known to occur only at high pressures.[3] Calcite is thermodynamically the most stable form of calcium carbonate at room temperature and at atmospheric pressure. The main difference between calcite, aragonite and vaterite lies in the arrangement of the ideally triangular CO_3^{2-} ions in their unit cells.[4] In rhombohedral and/or hexagonal calcite, the CO_3^{2-} sub-lattice is hexagonal and the triangular CO_3^{2-} ions are coplanar. The planes containing CO_3^{2-} ions are perpendicular to the *c*-axis and they are rotated by 60° from one CO_3^{2-} layer to the next. In the aragonite structure, although the CO_3^{2-} sub-lattice is hexagonal, the disposition of the CO_3^{2-} ions with respect to Ca^{2+} ions is different. A definitive crystal structure of the third polymorph vaterite is not as well understood as the other polymorphs. There is a general agreement that the unit cell of vaterite is hexagonal and CO_3^{2-} ions are aligned parallel to the *c*-axis and not perpendicular as in the case of calcite or aragonite.[5]

The use of $CaCO_3$ is increasing rapidly in a variety of areas like rubber, paint, paper, pharmaceuticals, cosmetics and dentifrices, wherein the surface properties play a very important role in the final product. Such studies have shown that Ca^{2+} and CO_3^{2-} are the most important surface ions in $CaCO_3$ dispersed in aqueous solutions. It has been suggested that H^+, OH^-, HCO_3^-, $[Ca(OH)]^+$ and $[Ca(HCO_3)]^+$ species are also present on the surface and influence the properties of the calcite surface.[6] Water undergoes physisorption and chemisorption by dissociatively adsorbing over the surface sites[7,8] generated by thermal decomposition and consequently changes the pore structure of calcite. In a recent FTIR study of the adsorption of H_2O and NH_3 on calcite,[9] the dissociative adsorption of water on calcite leading to the generation of hydroxyl and bicarbonate ions was proposed. All these studies strongly indicate the presence of CaO and/or $Ca(OH)_2$ type species on calcium carbonate surfaces.

The present paper describes the specific origin of hydroxyl ions on calcium carbonate surfaces and their quantitative estimation using variable temperature FTIR and molecular modelling studies. Calcium carbonates prepared by the carbonation of aqueous $Ca(OH)_2$ slurries under various experimental conditions, and those synthesised by double decomposition of $CaCl_2$ and Na_2CO_3 have been analysed, and the relative amounts of hydroxyl ions determined. The possibility of the formation of different types of hydroxyl ions in calcium carbonate lattices as well as their energetics of formation have been explored using molecular modelling studies.

Materials and methods

Synthesis

Calcium oxide (CaO) was obtained from Citurgia Chemicals Ltd. (India) and used as received. Calcium carbonate samples were prepared by the carbonation method,[10] in which CO_2 gas is bubbled through an aqueous slurry of $Ca(OH)_2$ under various controlled temperatures and different end pH conditions. Carbonation reactions were monitored by measuring the

Table 1 List of $CaCO_3$ samples prepared under different reaction conditions

Samples	Method of preparation	Reaction conditions		Calcite : aragonite ratio[a]
		Temperature/°C	End pH	
CHK-1	$Ca(OH)_2$ (aq.) + CO_2 (g)	30	7.0	69 : 31
CHK-2	$Ca(OH)_2$ (aq.) + CO_2 (g)	50	7.0	61 : 39
CHK-3	$Ca(OH)_2$ (aq.) + CO_2 (g)	30	9.0	62 : 38
CHK-4	$Ca(OH)_2$ (aq.) + CO_2 (g)	50	9.0	55 : 45
CHK-5	$CaCl_2 + Na_2CO_3$[b]	25	7.0	100% Calcite
CHK-6	$CaCl_2 + Na_2CO_3$[c]	80	7.0	100% Aragonite
CHK-7	$CaCl_2 + Na_2CO_3$[d]	25	—	40 : 60
CHK-8	$CaCl_2 + Na_2CO_3$[d]	25	—	70 : 30

[a]Calculated from the areas under the peaks at 873 and 854 cm^{-1} in the FTIR spectra. [b]Na_2CO_3 added to $CaCl_2$. [c]Simultaneous addition of $CaCl_2$ and Na_2CO_3. [d]$CaCl_2$ added to Na_2CO_3 in a different molar ratio.

pH of the aqueous slurry during the course of the reaction. Pure calcite and aragonite samples as well as intergrown calcite/aragonite samples were prepared by the solution method,[11] wherein aqueous $CaCl_2$ and Na_2CO_3 were combined in an equimolar ratio (double decomposition reaction). The experimental details regarding the preparation of samples investigated for the present study are listed in Table 1. All syntheses were performed in a jacketed stainless steel reactor of internal volume of 20 L.[12] Water was circulated through the jacket during the course of the experiment to maintain a constant reaction temperature.

The powder X-ray diffraction patterns were recorded on a Siemens D-5000 diffractometer using Cu-Kα ($\lambda = 1.5406$ Å) radiation. Routine FTIR spectra of the ground samples were recorded as KBr pellets using a Bomem FTIR spectrophotometer (Model: MB 102).

Temperature dependent Fourier transform infrared spectroscopy (FTIR)

In order to obtain spectra in the region of the carbonate framework vibrations, pressed pellets of the samples diluted with potassium bromide (0.6 mg in 300 mg) were used. Self supported calcium carbonate wafers were used in order to investigate the nature of surface hydroxyl ions. The preparation of self supported wafers involved processing the $CaCO_3$ samples under a pressure of 7 tons in^{-2} into thin wafers (5–7 mg cm^{-2}). A rectangular piece of wafer (1.5×1.2 cm) was mounted on a specially designed sample holder[13] and placed inside a FTIR transmittance cell positioned in the sample compartment of the spectrometer (Nicolet 60SXB). The cell was connected to a high vacuum system. The transmittance spectra were recorded after degassing the sample to 10^{-5} Torr at 100, 200, 300 and 400 °C for one hour each and, finally, after cooling to 100 °C. The spectra were recorded with 2 cm^{-1} resolution and averaged over 500 scans.

Molecular modelling

The atomic co-ordinates of the asymmetric unit cell of calcite were taken from a crystal structure study report.[14] The molecular models of the calcite crystal structure and the calcite 104 plane were generated using the Insight II Software package. The calcite lattice was modelled by considering a simulation box of $3 \times 3 \times 3$ unit cells. The 104 plane passing through the center of the simulation box was considered for studying the adsorption behaviour of water. The model of the calcite 104 surface has 9 layers, which takes care of the influence of the bulk on the adsorption characteristics of the surface. The energy minimization calculations were performed using the parameters derived for the simulation of bulk crystalline calcite. Hence, such calculations showed a phenomenological surface relaxation depending on the boundary conditions used to define the surface. The most stable surface of the calcite crystal, namely the calcite 104 plane, is known to undergo only a small relaxation relative to its bulk structure.[15,16] Hence, we have used in our studies a model of the calcite 104 plane with atoms fixed at their crystallographic locations. Such an approach has been successfully used to obtain isotherms and isosteric heats of adsorption of water.[17] A polarisable model of water as described earlier by other groups[17,18] has been used.

The interaction mode of water with the calcite 104 plane was derived using the energy minimization procedure. The interaction energy was calculated as the sum of the repulsive and attractive Lennard–Jones terms as well as the Coulombic terms, all of which are a function of the distance between atom pairs (r_{ij}) as shown in eqn. (1).

$$E_{\text{formation}} = \sum_i \sum_{j>i} [A_{ij}/{r_{ij}}^{12} - B_{ij}/{r_{ij}}^{6} + q_i q_j / r_{ij}] \quad (1)$$

The non-bonded interactions and the electrostatic interactions between the ions were calculated over the whole model. The energy of formation of surface hydroxyl ions was calculated according to eqn. (2) as shown below.

$$\text{Energy of formation of hydroxylated surface} = [E_{\text{hydroxylated calcite 104}}] - [E_{\text{calcite 104}} + E_{\text{water}}] \quad (2)$$

The Consistent Valence Force Field (CVFF) parameters of Dauber-Osguthorpe *et al.*[19] were used for the calculation of energy using the Discover software package. The Insight II and Discover software packages were developed and supplied by MSI, USA.[20] All calculations were carried out on a Silicon-Graphics-Indigo2 workstation.

Results and discussion

Synthesis

Precipitated calcium carbonate samples were prepared employing both the solution and the carbonation route, under different reaction conditions (Table 1). While the solution route leads to the isolation of pure calcium carbonate polymorphs, the formation of calcite/aragonite intergrowths is almost always observed when carbonation [eqn. (3)] is carried out in the temperature range 30–50 °C,[10] as are the samples considered in this study.

$$Ca(OH)_2 + CO_2 \rightarrow CaCO_3 + H_2O \quad (3)$$

$$CaCl_2 + Na_2CO_3 \rightarrow CaCO_3 + 2NaCl \quad (4)$$

In order to produce calcium carbonate samples with varying extents of surface hydroxyl ions for the current study, we synthesised four representative chalk samples (CHK-1, CHK-2, CHK-3 and CHK-4) by carefully controlling the extent of carbonation and the reaction temperature. These samples differ primarily in their phase compositions (calcite : aragonite ratio; Table 1) and possess different amounts of surface hydroxyl

ions. CHK-1 and CHK-2 were prepared using extended carbonation, with the anticipation that these samples would be devoid of any unreacted calcium hydroxide. CHK-3 and CHK-4 were deliberately prepared by terminating the carbonation at pH 9, so that these samples would contain some unreacted calcium hydroxide. Pure calcite (CHK-5) and aragonite (CHK-6) samples were synthesised adopting the solution route. Two calcite/aragonite intergrown samples with different calcite : aragonite ratios (CHK-7 and CHK-8) were also synthesized using the solution method, for comparison purposes.

Characterisation

FTIR spectra of $CaCO_3$ polymorphs display characteristic absorption bands in the region 1850–650 cm^{-1} corresponding to the four types of C–O bond vibrations, namely symmetric stretching (ν_1), out-of-plane bending (ν_2), a doubly degenerate asymmetric stretching (ν_3) and a doubly degenerate in-plane bending (ν_4).[21] The symmetric stretching mode ν_1 is infrared inactive, hence, only three bands due to ν_2, ν_3 and ν_4 are observed in the FTIR spectrum of calcite at 873, 1440 and 710 cm^{-1}, respectively. On the other hand, all the six fundamental frequencies are permitted in aragonite because of the non-degeneracy of the ν_3 and ν_4 bands due to the reduction in symmetry. In our infrared measurements, aragonite displayed five well-resolved bands at 700, 712, 854, 1080 and 1480 cm^{-1}, and a shoulder-like feature at 1420 cm^{-1}.

Phase compositions of calcite and aragonite in calcium carbonate samples prepared following the carbonation and the solution methods are described in Table 1. The relative amounts of calcite and aragonite were calculated from the ratio of the areas under the 873 and 854 cm^{-1} bands in their infrared spectra. This was then compared with the results obtained from their X-ray powder diffraction patterns. The area under the principal XRD line at 3.03 Å (104 plane) for calcite and 3.39 Å (111 plane) for aragonite were used to quantify the relative amounts of calcite and aragonite in these calcium carbonate samples.[22] The calcite : aragonite ratios calculated from the FTIR and XRD methods are in good agreement.

Temperature dependent FTIR studies

In order to gain insight into the origin of hydroxyl ions in calcium carbonate, the samples were subjected to temperature dependent FTIR investigations. FTIR spectra of these samples were acquired on their self supported wafers at 100, 200, 300 and 400 °C respectively, followed by cooling to 100 °C under vacuum. Fig. 1 displays the temperature dependent FTIR spectra of CHK-1, CHK-2, CHK-3 and CHK-4 samples. The spectra of all the samples exhibited two well-defined sharp bands at 3690 and 3640 cm^{-1} attributed to hydroxyl stretching (ν_{OH}) and referred to as Type I and Type II hydroxyl ions, respectively. The integrated intensities of bands under the 3690 and 3640 cm^{-1} peaks in all of the spectra are summarised in Table 2.

As can be noted from Table 2, all four samples display both 3690 and 3640 cm^{-1} bands with varying relative intensities. The intensities of the 3690 cm^{-1} band (Type I) in CHK-3 and CHK-4 are significantly higher than those in CHK-1 and CHK-2. Upon heating to 400 °C, the 3690 cm^{-1} band disappeared and did not re-appear upon cooling back to 100 °C. On the other hand, the 3640 cm^{-1} band (Type II) in all samples did not disappear upon heating to 400 °C and was found to persist even upon cooling to 100 °C. This band disappeared only when calcium carbonate samples were heated to *ca.* 700 °C, corresponding to its decomposition to calcium oxide. In addition, with increasing temperature, the broad band centred at 3550 cm^{-1} (Fig. 1) which is due to adsorbed

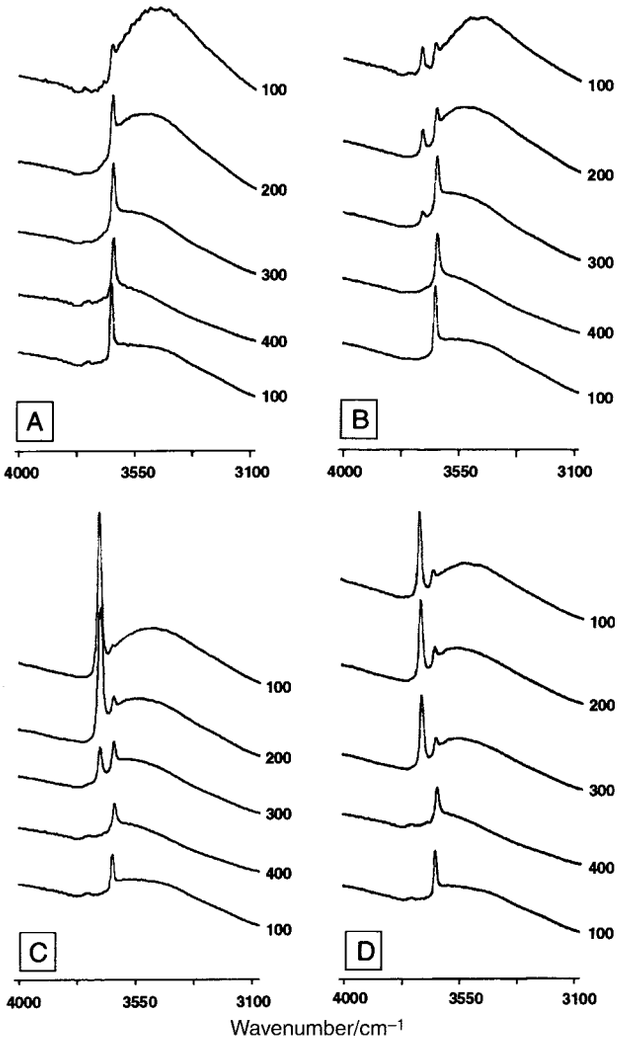

Fig. 1 Temperature dependent FTIR spectra of (A) CHK-1, (B) CHK-2, (C) CHK-3 and (D) CHK-4. For each sample, spectra were recorded at 100, 200, 300 and 400 °C and, finally, cooled back to 100 °C. The *y*-axis shows the absorbance (arbitrary units).

water and –OH species perturbed due to hydrogen bonding was found to decrease in intensity because of desorptive losses.

Clearly and unambiguously, the Type I hydroxyl species correspond to unreacted $Ca(OH)_2$ since both of these have very similar thermal decomposition profiles. In order to substantiate this, an independent FTIR study was carried out with $Ca(OH)_2$ and it exhibited similar behaviour. The intense bands at *ca.* 3690 cm^{-1}, not shown in Fig. 1 (pattern matches that reported in the literature),[23] vanished upon heating to 400 °C, and no bands were found to re-appear after cooling to 100 °C. At this temperature, $Ca(OH)_2$ is known to decompose to CaO irreversibly, and thus, upon cooling to 100 °C the spectrum remained unchanged. It is interesting to note that CHK-1 and CHK-2 were prepared by carbonating $Ca(OH)_2$ slurries till an end pH of 7 was attained and thus the intensities of Type I hydroxyl bands in these two samples are very low, suggesting the presence of extremely small amounts of unreacted $Ca(OH)_2$. As CHK-3 and CHK-4 were prepared at an end pH of 9, a significant amount of unreacted $Ca(OH)_2$ was present in these samples as evident from the presence of very intense Type I hydroxyl bands.

The Type II hydroxyl species which appear at 3640 cm^{-1} in the FTIR spectra are ascribed to those present as interstitial defects and strongly associated with the calcium carbonate lattice. The nature of interstitial defects has been analysed using molecular modelling as presented in the following section. They are believed to be strongly associated with the $CaCO_3$ lattice,

Table 2 Relative concentration of hydroxyl ions

Samples	Area of peak under 3640 cm^{-1} (Type II = interstitial hydroxy ion) after evacuation at the following temperatures/cm^{-1}					Area of peak under 3690 cm^{-1} (Type I = unreacted $Ca(OH)_2$) after evacuation at the following temperatures/cm^{-1}				
	100 °C	200 °C	300 °C	400 °C	100 °C[a]	100 °C	200 °C	300 °C	400 °C	100 °C[a]
CHK-1	3.8[b]	7.9	9.5	8.9	9.1	1.1	0.9	0.7	0	0
CHK-2	2.5[b]	3.7	7.5	6.9	7.2	2.8	1.2	0	0	0
CHK-3	0.6[b]	2.3	4.4	4.7	4.8	23.8	17.3	4.8	0	0
CHK-4	*ca.* 1[b]	*ca.* 1[b]	*ca.* 2[b]	4.8	7.5	12.8	12.0	6.6	0	0

[a]Cooled back from 400 °C. [b]Deconvolution was not possible due to the interference from the broad water band. Hence, the area was determined by integrating the area between peak minima, before baseline correction.

because they do not disappear even after heating to 400 °C under vacuum (Fig. 1). The rationale for this is that these bands only disappear when $CaCO_3$ undergoes self-decomposition. This phenomenon occurs possibly *via* a mechanism of replacement of CO_3^{2-} by OH^- ions in the $CaCO_3$ framework. It is also interesting to note from Table 2 that the intensity of Type II hydroxyl ions increases with increasing temperature up to 300 °C and then reaches a plateau even after cooling to 100 °C. During this process, the intensity of adsorbed water also decreases. Thus, it can be surmised that $CaCO_3$ surfaces promote the hydrolysis reaction at an elevated temperature especially at the defect sites (Type II hydroxyl) present on the $CaCO_3$ surface. Similar phenomena of the dissociation of water on defect sites of NaCl crystal surface and certain Ca^{2+}/La^{3+} exchanged zeolites are also known.[24]

Temperature dependent FTIR spectra of pure calcite (CHK-5) and aragonite (CHK-6) samples as well as their intergrowths (CHK-7), prepared by the solution method are displayed in Fig. 2. There are no structural hydroxyl ions in these samples as can be seen from the figure. A similar study could not be conducted on a pure vaterite sample, because on heating to 200 °C the sample became almost opaque to the IR beam. These results indicate and substantiate the fact that $CaCO_3$ samples prepared by the solution route do not exhibit either Type I or Type II hydroxyl ions irrespective of the crystal phase formed. Therefore, these types of hydroxyl ions originate when $CaCO_3$ is prepared by the carbonation method only, wherein the reaction is between a strong base and a weak acid.

Modelling the interaction of water with the calcite 104 plane

Fig. 3 shows a molecular graphics picture of a calcite lattice. Several crystal planes are also marked. This figure indicates the heterogeneity of atom distribution in each of these planes as well as their frequency of occurrence. Although there have been several studies[25–27] on the application of computational methods to understand the bulk and surface characteristics of calcite, only a few reports[28,29] deal with the interactions of small molecules with calcite surfaces. The hydroxyl ions were found to be present only in the $CaCO_3$ samples prepared by the carbonation method (CHK-1 to CHK-4). In all these samples, the calcite : aragonite ratio is always greater than 1.0 as shown in Table 1. Hence, an elaborate modelling of the nature, origin and stability of the surface hydroxyl ions on the calcite 104 plane was undertaken.

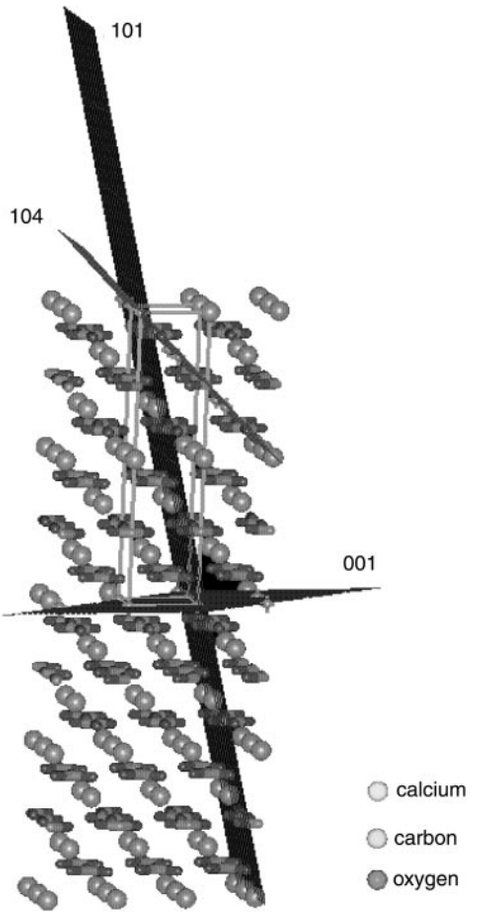

Fig. 3 A molecular graphics picture of the calcite lattice viewed down the 010 plane. The unit cell of calcite ($4.989 \times 4.989 \times 17.060$ Å) is also inscribed to indicate the relative positions of different surfaces. The 104 plane, 101 plane and 001 plane are also shown to indicate the density of atoms in different Miller index planes. The coordination between Ca^{2+} and O^{2-} ions is not shown and CO_3^{2-} ions are shown as single units for better visualisation.

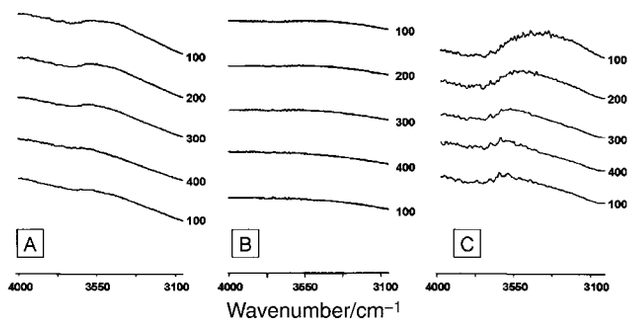

Fig. 2 Temperature dependent FTIR spectra of (A) CHK-5, (B) CHK-6 and (C) CHK-7. For each sample, spectra were recorded at 100, 200, 300 and 400 °C and, finally, cooled back to 100 °C. The *y*-axis shows the absorbance (arbitrary units).

The favourable mode of adsorption of water over the calcite 104 plane was derived by minimizing the interaction energy. A utility code was used to generate several starting orientations of water over the 104 plane. A grid having an interval of 0.5 Å over an area of 6.0 Å × 5.0 Å on the calcite 104 plane was created. The water molecule was placed at each of the 120 (12×10) locations at the grid points generated as above. The initial orientation of the water molecule was chosen in such a way that the molecular plane (the plane containing the three atoms of the water molecule) is parallel to the calcite 104 plane. The water molecule was rotated in the *x*, *y* and *z* directions by

90° considering the molecular plane as the *xy* plane and *z* as the direction perpendicular to the *xy* plane.

For each orientation of the water molecule at the grid points, energy minimization was adopted to deduce the stable modes of adsorption of water. The interaction energy between the calcite 104 surface and the water molecule was minimized with respect to the internal degrees of freedom of water as well as the non-bonding interactions. All atoms of the calcite 104 surface were constrained to their crystallographic positions with the calcium and carbonate ions maintained at their full ionic charges (+2 and −2, respectively). The carbonate charge was partitioned between carbon (+0.919) and oxygen (−0.973). The oxygen atom (−0.4) and the hydrogen atoms (+0.2) of the water were considered to be partially charged.[30] The potential parameters used in the calculation are given in Table 3.

Following the above procedure, two stable modes of adsorption of water over carbonate species were identified. In mode I, the water molecule adsorbs over CO_3^{2-} leading to two hydroxyl groups, which may be initially formed through hydrogen bonding, as shown in eqn. (5).

$$CO_3^{2-} + H_2O \rightarrow CO_2 + 2[OH]^- \quad (5)$$

This process leads to the formation of $Ca(OH)_2$ type species on the surface with the evolution of CO_2. The molecular picture of the hydroxylated surface corresponding to the observed IR band at 3690 cm^{-1} (Type I) is shown in Fig. 4. The energy of formation of this species is calculated according to eqn. (2) and listed in Table 4. In mode II, the water molecule adsorbs over CO_3^{2-}, by forming a single hydrogen bond as shown in eqn. (6).

$$CO_3^{2-} + H_2O \rightarrow HCO_3^- + OH^- \quad (6)$$

This process leads to the formation of calcium bicarbonate and hydroxide ion on the surface. Thus, the molecular picture of the hydroxylated surface corresponding to the observed IR band at 3640 cm^{-1}(Type II) is also derived. The energy of formation for this species is also calculated according to eqn. (2) and listed in Table 4. As observed from Table 4, the formation of a hydroxyl and a bicarbonate ion [process shown in eqn. (6)] is energetically more favourable than the formation of two hydroxyl ions [process shown in eqn. (5)].

We also considered exploring the feasibility of multiple substitution processes in the calcium carbonate lattice and specifically we modelled the replacement of more than one carbonate ion by hydroxyl and bicarbonate ions on the calcite 104 surface. This exercise was performed to find out the preferred number of surface hydroxyl ions that can be accommodated on the 104 plane. For this purpose, the following three possibilities of distribution of hydroxyl and bicarbonate ion pairs in (i) neighbouring (adjacent) positions, (ii) next neighbouring positions, and (iii) non-neighbouring positions, were considered, as shown in Fig. 5(a–c). The energies of formation of the hydroxylated surface corresponding to the above situations are also included in Table 4. The energy of formation of a pair of hydroxyl and bicarbonate ions is obviously favourable, but when these are partitioned for the first and second set, the energy of formation for the second set is relatively unfavourable. The energy of formation for the second set is phenomenally dependent on its position with respect to the first set. It was found that the formation of the second pair of ions in the non-neighbouring position (Fig. 5c) [−160.79–(−87.42) kJ mol^{-1}] is almost as favourable as the formation of two hydroxyl ions replacing a carbonate ion [eqn. (5), Fig. 4]. However, the formation of a second pair of hydroxyl and bicarbonate ions in next-neighbouring positions (Fig. 5b) [−157.37–(−87.42) kJ mol^{-1}] and the adjacent positions (Fig. 5a) [−124.33–(−87.42) kJ mol^{-1}] was found to be relatively unfavourable. Considering the fact that the hydroxyl ions are formed between the carbonate ions and the distances between the carbonate ions in the perpendicular directions are 4.05 and 4.99 Å, the formation of two hydroxyl ions in non-neighbouring positions (Fig. 5c) leads to the formation of two surface hydroxyl ions over a surface area of 1.0 nm^2. It is observed that even the formation of hydroxyl groups in adjacent

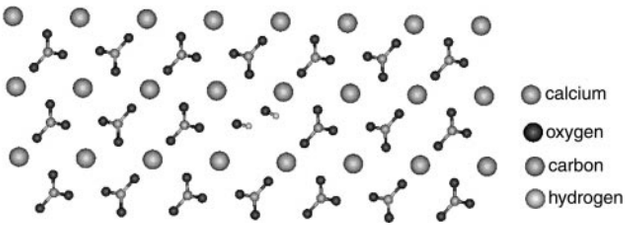

Fig. 4 A molecular graphics picture of the calcite 104 plane, where a CO_3^{2-} ion is substituted by two OH^- ions. The picture shows a cross-sectional view of the 104 plane.

Table 3 Parameters used in the energy minimization calculations

Bond length parameters: $E = K_1(r - r_o)^2$

Atom[a]	Atom[a]	r_0/Å	K_1/kcal mol^{-1} $Å^{-2}$
O	H	0.96	540.6336

Bond angle parameters: $E = K_2(\Theta - \Theta_0)^2$

Atom[a]	Atom[a]	Atom[a]	Θ_0/degrees	K_2/kcal mol^{-1} $degree^{-2}$
H	O	H	104.5	50.0000

Nonbonded parameters: $E = A_{ij}/r^{12} - B_{ij}/r^6$, where $A_{ij} = (A_iA_j)^{1/2}$; $B_{ij} = (B_iB_j)^{1/2}$

Atom	A/kcal mol^{-1} $Å^{12}$	B/kcal mol^{-1} $Å^6$
O	629358.000	625.500
H	0.00000001	0.000
Ca^{2+}	119025.000	240.25
O^{2-}	272894.785	498.878
C	2968753.359	1325.708

[a]Atom types: O, oxygen of water; H, hydrogen of water; Ca^{2+}, calcium of calcium carbonate; O^{2-}, oxygen of carbonate; C, carbon of carbonate.

Table 4 Energetics for the formation of different types of hydroxylated calcite (104) plane

Type of hydroxyl ion	Energy of formation/kJ mol^{-1}
Two hydroxyl ions replacing the carbonate ion [eqn. (5); Fig. 4]	−73.60
One hydroxyl and one bicarbonate ion replacing the carbonate ion [eqn. (6)]	−87.42
Two hydroxyl and two bicarbonate ions replacing two carbonate ions in adjacent (neighbouring) positions (Fig. 5a)	−124.33
Two hydroxyl and two bicarbonate ions replacing two carbonate ions in next-neighbouring positions (Fig. 5b)	−157.37
Two hydroxyl and two bicarbonate ions replacing two carbonate ions in non-neighbouring positions (Fig. 5c)	−160.79

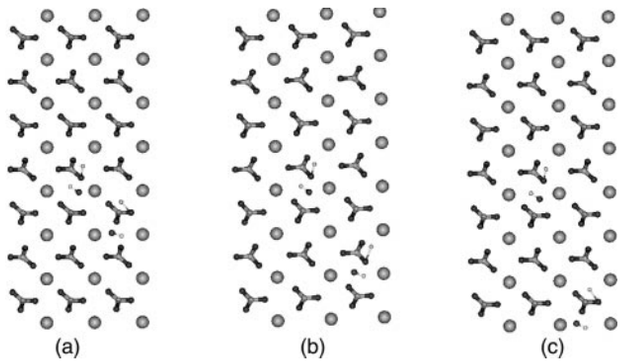

Fig. 5 Molecular graphics pictures of the calcite 104 plane, where two CO_3^{2-} ions are substituted by two sets of OH^- and HCO_3^- ions. Three possibilities of hydroxyl and bicarbonate ion formation are shown: (a) neighbouring (adjacent) positions, (b) next neighbouring positions and (c) non-neighbouring positions. The labelling of atoms is same as in Fig. 4.

positions is still exothermic, which indicates that the physisorption of more water molecules is feasible. This result is again in agreement with the temperature dependent FTIR results, wherein a broad band at 3550 cm^{-1} due to physisorbed water (Fig. 1) disappeared with increasing temperature. The energy of formation of hydroxyl ion is dependent on the distance between the existing and the newly forming hydroxyl ions. Qualitatively, the layer to layer distance as well as the ion to ion distance are the factors controlling the formation of hydroxyl ions and similar arguments hold good for other planes of different phases of $CaCO_3$. More accurate quantum chemical calculations are being undertaken to study the relaxation of surface atoms nearer to hydroxyl ions in order to obtain accurate energetics and a better understanding of the activation energy barrier for the dissociation mechanism of the chemisorbed water.

Conclusions

We have probed the origin and nature of hydroxyl ions in $CaCO_3$ by variable temperature FTIR and molecular modelling studies. FTIR studies show the presence of hydroxyl ions (3690 cm^{-1} band) arising due to an incomplete carbonation reaction. The band at 3640 cm^{-1} is ascribed to hydroxyl ions strongly bound to the $CaCO_3$ lattice. These lattice bound hydroxyl ions exhibit an unusually high thermal stability and are stable up to temperatures at which $CaCO_3$ starts undergoing self-decomposition to its corresponding oxide. However, samples of pure calcite and aragonite, as well as their intergrowths, prepared by the solution route do not possess any such hydroxyl ions.

The potential interactions of the water molecules over the calcite 104 surface have been considered and molecular modelling studies were performed on such hydroxylated surfaces. The energy of formation of hydroxylated surfaces at low surface coverage of water corroborates well with the results obtained from temperature dependent FTIR studies. The highlights of the molecular modelling studies are: (i) that the replacement of a carbonate ion by a surface hydroxyl and a bicarbonate ion is energetically more favourable than replacement by two hydroxyl ions, and (ii) formation of a maximum of two surface hydroxyl ions over a surface area of 1.0 nm^2 is predicted.

References

1 L. Brecevic and A. E. Nielosen, *J. Cryst. Growth*, 1989, **98**, 504.
2 J. R. Clarkson, T. J. Price and C. J. Adams, *J. Chem. Soc., Faraday Trans.*, 1993, **88**, 243.
3 L. Merrill and W. A. Bassett, *Acta Crystallogr., Sect. B*, 1975, **31**, 343.
4 H. J. Meyer, *Z. Kristallogr.*, 1969, **128**, 183.
5 G. Behrens, L. T. Kuhn, R. Ubic and A. H. Heuer, *Spectrosc. Lett.*, 1995, **28**, 983.
6 D. W. Thomson and P. G. Pownall, *J. Colloid Interface Sci.*, 1989, **131**, 74.
7 R. B. Gamage and S. J. Gregg, *J. Colloid Interface Sci.*, 1972, **38**, 118.
8 R. B. Gamage, *Colloid Interface Sci. (Proc. 50th Int. Conf.)*, 1976, **3**, 1.
9 W. Negale and C. H. Rochester, *J. Chem. Soc., Faraday Trans.*, 1990, **86**, 181.
10 V. A. Juvekar and M. M. Sharma, *Chem. Eng. Sci.*, 1973, **28**, 825.
11 J. L. Wray and F. Daniels, *J. Am. Chem. Soc.*, 1957, **79**, 2031.
12 D. Chakrabarty and S. Mahapatra, *J. Mater. Chem.*, 1999, **9**, 2953.
13 S. G. Hegde, R. Kumar, R. N. Bhat and P. Ratnasamy, *Zeolites*, 1989, **9**, 233.
14 R. W. G. Wyckoff, *Crystal structures*, Interscience Publishers, New York, 1964, vol. 2, pp. 362–364.
15 Y. Liang, A. S. Lea, D. R. Baer and M. H. Engelhard, *Surf. Sci.*, 1996, **351**, 172.
16 N. H. de Leeuw and S. C. Parker, *J. Phys. Chem. B*, 1998, **102**, 2914.
17 E. Stockelmann and R. Hentschke, *Langmuir*, 1999, **15**, 5141.
18 S. W. Rick and B. J. Berne, *J. Am. Chem. Soc.*, 1996, **118**, 672.
19 P. Dauber-Osguthorpe, V. A. Roberts, D. J. Osguthorpe, J. Wolff, M. Genest and A. T. Hagler, *Proteins: Struct., Funct., Genet.*, 1988, **4**, 31.
20 INSIGHT II and DISCOVER software packages, Version 400, Molecular Simulations Inc., USA, 1997.
21 A. G. Xyla and P. G. Koutsoukos, *J. Chem. Soc., Faraday Trans. 1*, 1989, **85**, 3165.
22 C. G. Kontoyannis, N. G. Orkoula and P. G. Koutsoukos, *Analyst*, 1997, **122**, 33.
23 O. Oehler and H. H. Gunthard, *J. Chem. Phys.*, 1968, **48**, 2036.
24 D. J. Dai, S. J. Peters and G. E. Ewing, *J. Phys. Chem.*, 1995, **99**, 10299.
25 H. H. Adler and P. F. Kerr, *Am. Mineral.*, 1962, **47**, 700.
26 N. H. de Leeuw and S. C. Parker, *J. Chem. Soc., Faraday Trans.*, 1997, **93**, 467.
27 S. C. Parker, P. M. Oliver, N. H. de Leeuw, J. O. Titiloye and G. W. Watson, *Phase Transitions*, 1997, **61**, 83.
28 D. Kralj, L. Brecevic and A. E. Nielson, *J. Cryst. Growth*, 1990, **104**, 793.
29 J. R. Clarkson, T. J. Price and C. J. Adams, *J. Chem. Soc., Faraday Trans.*, 1992, **188**, 243.
30 K. L. Nagy, R. T. Cygnan, C. S. Scotto, C. J. Brinker and C. S. Ashley, *Mater. Res. Soc. Symp. Proc.*, 1997, **462**, 301.